

## 17.5 A mm-Sized Implantable Power Receiver with Adaptive Link Compensation

Stephen O'Driscoll, Ada S. Y. Poon, Teresa H. Meng

Stanford University, Stanford, CA

Wireless powering of implanted devices obviates the need for batteries, which must be periodically replaced and constitute a health risk. There has long been an assumption that efficient wireless transfer of power to biomedical implants requires fields operating in the low MHz in order to avoid excess losses in tissue, thus requiring antenna diameters of a few cm [1]. Such antennae increase device size and thereby restrict the range of viable applications. This work presents a wireless power transfer system that uses an antenna area 100× smaller than previous designs [2] while maintaining the same power transfer efficiency over the same range.

Our theoretical investigation [3] has shown that the optimal transmission frequency is in the GHz range for infinitesimally small antennae:

$$\omega_{opt} \approx \sqrt{\frac{c\sqrt{\epsilon_{r,0}}}{d\tau(\epsilon_{r,0} - \epsilon_{\infty})}} \quad (1)$$

provided  $d\epsilon_{r,0}^{1.5} \gg c\tau(\epsilon_{r,0} - \epsilon_{\infty})$ , where  $d$  is the transmit-receive antenna separation,  $\epsilon_{r,0}$  and  $\epsilon_{\infty}$  are the relative permittivities of the tissue at dc and infinite frequencies,  $\tau$  is the tissue relaxation time constant, and  $c$  is the speed of light in a vacuum. In practical systems antennae have finite size and the tissue is multi-layered (skin, fat, muscle, etc). Incorporating those additional factors gives an optimal frequency of approximately 1GHz for a 2×2cm<sup>2</sup> square loop transmit antenna and a 2×2mm<sup>2</sup> square loop receive antenna at a separation of 15mm of layered tissue, to achieve a theoretical maximum link gain of -31dB. This work presents such a link operating at 915MHz, implementing the power receiving circuits in 0.13µm CMOS. Figure 17.5.1 illustrates the physical dimensions and a block diagram of the power transfer system.

A wavelength in tissue,  $\lambda$ , is about 50mm at 915 MHz. Neither near field,  $d \ll \lambda$ , nor far field,  $d \gg \lambda$ , conditions hold and neither antenna matching, as used in far-field links, nor resonant tuning, as used in near field links [2], [4], can deliver within 10dB of the theoretical maximum gain. We propose *simultaneous conjugate matching* to accomplish this goal.

Link parameters cannot be known accurately prior to deployment due to variation in implant depth; misalignment between antennae; and variation in tissue composition. Hence the required match components cannot be known exactly. Simulated normalized  $|V_L|$ , the magnitude of the voltage across the resistive portion of the load, versus the receive match shunt capacitance,  $C_2$ , is shown in Fig. 17.5.2(a).  $|V_L|$  has a maximum at  $C_{2,opt} = 4.02$ pF and falls off sharply as  $C_2$  varies. In fact, if  $C_2$  varies by 2.5% from the design value, i.e.  $C_2 = 3.91$ pF, then  $|V_L|$  falls to 65% of the maximum.

An adaptive matching circuit is proposed to overcome link sensitivity.  $|V_L|$  has a global maximum as a function of  $C_2$ . Therefore gradient search techniques can be used:

$$C_{2,k+1} = C_{2,k} + \mu \cdot \text{fn}(\nabla_k) \quad \text{where} \quad \nabla_k = \left. \frac{\partial |V_L|}{\partial C_2} \right|_{C_2=C_{2,k}} \quad (2)$$

The first partial derivative of  $|V_L|$  with respect to  $C_2$ , becomes very large near the optimum, so iterating with step size proportional to  $\nabla_k$ , e.g. LMS, would be unstable. Instead a hybrid of binary and gradient search is used to drive  $C_2$  to the optimum value. The algorithm is summarized in Fig. 17.5.2(c).

A surface-plot of  $|V_L|$  versus receive match components, Fig. 17.5.2(b), shows that there is only one degree of freedom. The tunable match is therefore realized using a fixed inductance and a digitally controlled nine-element binary-weighted MiM capacitor array, shown in Fig 17.5.2(d). Each of the capacitors in the array is selectable apart from the 2°C capacitance which is permanently connected. At startup all of the switches are open and  $C_2 = 3.7$ pF, ensuring that the 3-stage rectifier output  $\geq 0.7$ V for all antennae separation from 7.2mm to 19.1mm. This voltage is used as the supply for the array switches. The sign of  $\nabla_k$  is found by switching the smallest capacitance in and out of the array.

In this prototype the capacitor array and digital control are implemented on chip but the adaptation algorithm is run off-chip.  $C_2$  converges to the optimum value within 18 steps. Transmit and receive matches can be tuned separately.

A CMOS rectifier using diode connected MOSFETs with  $V_{TH} \geq 0.4$ V would generate an output voltage  $V_{DC} \leq 0.35$ V for input amplitude  $V_{IN} = 0.75$ V. Therefore five or six such stages would be needed to produce an output which could be reliably regulated to 1.2V, incurring unacceptable loss. Instead a synchronous self-driven rectifier is used [5,6]. Consider a single rectifier stage in Fig. 17.5.3. When node A is high  $M_0$  and  $M_2$  are "on" and  $M_1$  and  $M_3$  are "off". The applied gate-source voltage may not be enough to turn the devices strongly on or off but provided  $R_{OFF} \gg R_L \gg R_{ON}$  current will be steered to the load through opposite paths each half-cycle and a rectified voltage of  $V_{REC} = V_{IN} \cdot R_L / (R_L + R_{ON})$  produced. This design is more efficient than using diode-connected devices for rectification if the voltage drop due to forward conduction loss,  $V_{IN} \cdot R_{ON} / (R_{ON} + R_L)$ , is less than  $V_{TH}$ .

When the sinusoidal input falls below the dc output, the nominally "on" devices experience reverse conduction loss. Since  $V_{IN}$  has similar magnitude to  $V_{TH}$ , the "on" and "off" resistances are relatively close to  $R_L$  for a significant portion of each cycle and the nominally "off" devices shunt current away from the load. As W/L is increased  $R_{OFF}$  and  $R_{ON}$  decrease, reducing forward conduction loss, but increasing reverse and "off" state conduction loss. Therefore an optimum set of W/L exists which minimizes total loss. The various loss currents are illustrated with simulated performance of a single stage, Fig. 17.5.3(c). In this link the input amplitude seen by the rectifier is about 0.75V and each rectifier stage, optimally sized, has a  $V_{DROP}$  of 0.15V. Three stages are connected in a charge pump configuration with a 1pF pumping capacitance, chosen to equal the output smoothing capacitance. The measured rectifier efficiency is 65%. A simple series regulator is used to give a 1.2V supply, Fig. 17.5.4. The first replica feedback is used to generate the gate bias, desensitizing gate control to load switching. A second replica bias and control loop maintains a minimum current of 15 A through the series regulating FET.

The power receiver was implemented in 0.13µm CMOS and bonded to a 2×2mm<sup>2</sup> loop antenna with controlled bond wire length used as inductance  $L_2$ . A 2×2cm<sup>2</sup> loop was used as the transmit antenna and the antennae were separated by 15mm of bovine muscle tissue. Measured rectifier and regulator output voltages versus load impedance and antenna separation are shown in Fig. 17.5.5. Regulator output of 1.2V ± 1% is maintained as the current load varies from 15µA to 120µA and as the range varies from 7.5mm to 17.5mm. A 3.5dB gain is achieved by adaptive matching for a receiver at 1mm range displacement plus 1mm of axial mis-alignment. The performance is summarized in Fig. 17.5.6.

This work has demonstrated the application of simultaneous conjugate matching to wireless power transfer links to realize maximum theoretical gain; adaptive matching circuitry to compensate for link variations; and a high efficiency rectifier.

### Acknowledgements:

The authors acknowledge the generous fabrication support of TSMC and the Lu Stanford Graduate Fellowship.

### References:

- [1] W. Heetderks, "RF Powering of Millimeter- and Submillimeter-Sized Neural Prosthetic Implants," *IEEE Trans. Biomedical Engineering*, pp. 323-327, May 1988.
- [2] C. Sauer, et al., "Power Harvesting and Telemetry in CMOS for Implanted Devices," *IEEE Trans. Circuits and Systems-I*, pp. 2605-2613, Dec. 2005.
- [3] A. S. Y. Poon, S. O'Driscoll, and T. H. Meng, "Optimal Operating Frequency in Wireless Power Transmission for Implantable Devices," *Proc. IEEE Engineering in Medicine and Biology Society Annual International Conference (EMBC)*, pp. 5673-5678, Aug. 2007.
- [4] N. Donaldson, and T. Perkins, "Analysis of resonant coupled coils in the design of radio-frequency transcutaneous links," *Journal of Medical and Biological Engineering and Computing*, pp. 612-627, Sept. 1983.
- [5] M. Zhang, and F. Lee, "Commutation analysis of self-driven synchronous rectifiers in an active-clamp forward converter," *IEEE Power Electronics Specialists Conference*, pp. 868-873, June 1996.
- [6] S. Mandal, and R. Sarpeshkar, "Low-Power CMOS Rectifier Design for RFID Applications," *IEEE Trans. Circuits and Systems-I*, pp. 1177-1188, June 2007.

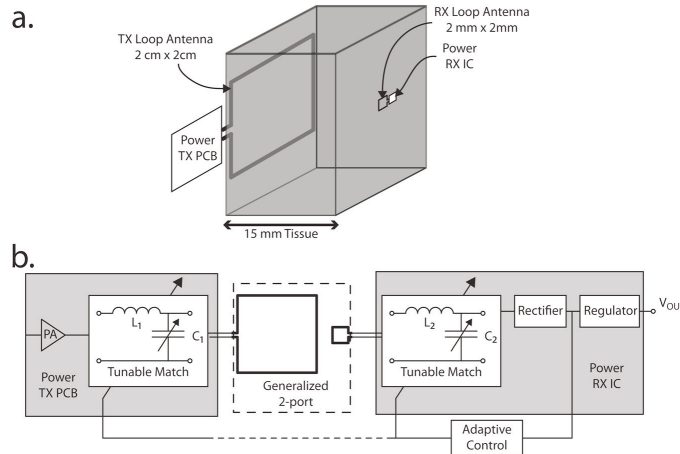


Figure 17.5.1: a. Scale representation of transmit and receive antenna and their separation. b. Block diagram of the power transfer system.

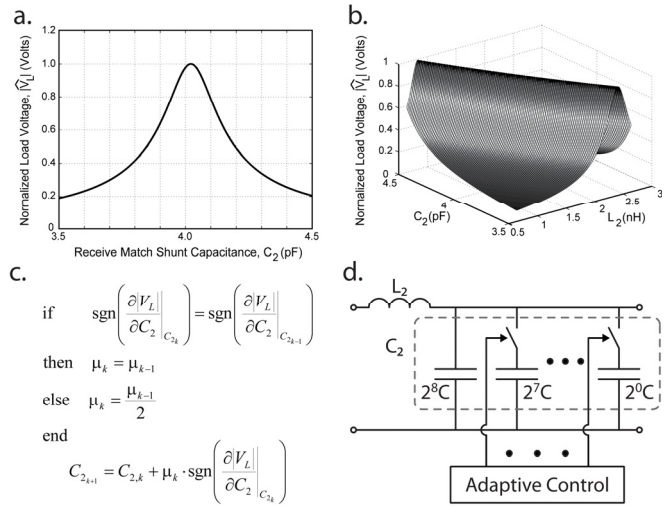


Figure 17.5.2: a. Normalized load voltage variation with match capacitance. b. Normalized load voltage variation with match capacitance and inductance. c. Adaptation algorithm. d. Digitally controlled tunable match (receive side).

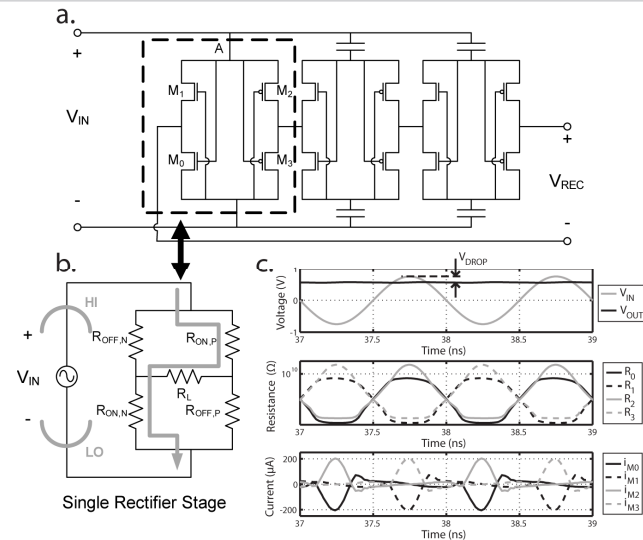


Figure 17.5.3: a. 3-stage self-synchronous rectifier. b. Principle of operation of a single stage. c. Simulated voltage drop and conduction losses of a single stage.

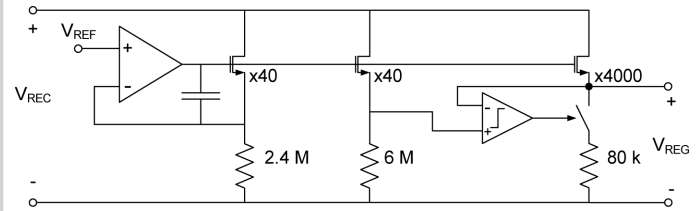


Figure 17.5.4: Regulator schematic.

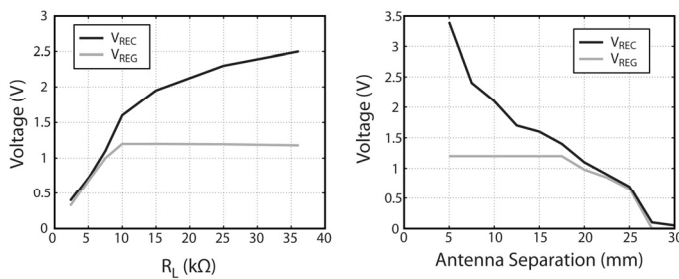


Figure 17.5.5: Measured rectifier and regulator output voltages versus load impedance and antenna separation.

Tx Antenna Size	2cm x 2cm	
Tx Power	0.25W	
Operating Frequency	915MHz or 1GHz	
Inter-Antenna Dielectric	15mm, Bovine Muscle Tissue	
Rx Antenna Size	2mm x 2mm	
Technology	0.13µm CMOS	
Area	0.37mm <sup>2</sup>	
Startup Time	4µs	
<b>For nominal 12 kΩ load on regulator output:</b>		
Rectifier Efficiency	65%	
Regulator Efficiency	75%	
Gain of Link + Rectifier + Regulator	-33.2dB	
Theoretical Maximum Link Gain (ac out)	-31.0dB	
DC Power Out	140µW @ 1.2V regulated	
<b>Adaptation Performance:</b>		
<b>Rx Placement</b>	<b>Matching</b>	<b>Gain (dB)</b>
Ideal	Adaptation ON	-32.1
+1mm range	Adaptation OFF	-35.8
+1mm range	Adaptation ON	-32.3
+1mm misalignment		
Range (for V <sub>REG</sub> = 1.2V +/- 1%)		7.5mm to 17.5mm

Figure 17.5.6: Performance summary.

ISSCC 2009 PAPER CONTINUATIONS

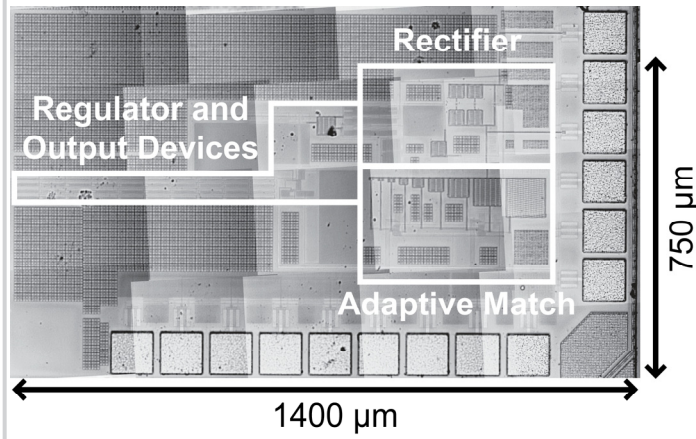


Figure 17.5.7: Die micrograph.